



Published in final edited form as:

*Results Probl Cell Differ.* 2010 ; 52: 147–157. doi:10.1007/978-3-642-14426-4\_12.

## The Olfactory Bulb: A Metabolic Sensor of Brain Insulin and Glucose Concentrations via a Voltage-Gated Potassium Channel

**Kristal Tucker,**

Program in Neuroscience, The Florida State University, Tallahassee, FL, USA

**Melissa Ann Cavallin,**

Program in Neuroscience, The Florida State University, Tallahassee, FL, USA

**Patrick Jean-Baptiste,**

Program in Neuroscience, The Florida State University, Tallahassee, FL, USA

**K.C. Biju,**

Program in Neuroscience, The Florida State University, Tallahassee, FL, USA

**James Michael Overton,**

Program in Neuroscience, The Florida State University, Tallahassee, FL, USA

**Paola Pedarzani,** and

Research Department of Neuroscience, Physiology and Pharmacology, University of College, London, London, UK

**Debra Ann Fadool**

Program in Neuroscience, The Florida State University, Tallahassee, FL, USA

Institute of Molecular Biophysics, The Florida State University, Tallahassee, FL, USA

Debra Ann Fadool: dfadool@bio.fsu.edu

### Abstract

The voltage-gated potassium channel, Kv1.3, contributes a large proportion of the current in mitral cell neurons of the olfactory bulb where it assists to time the firing patterns of action potentials as spike clusters that are important for odorant detection. Gene-targeted deletion of the Kv1.3 channel, produces a “super-smeller” phenotype, whereby mice are additionally resistant to diet- and genetically-induced obesity. As assessed via an electrophysiological slice preparation of the olfactory bulb, Kv1.3 is modulated via energetically important molecules – such as insulin and glucose – contributing to the body’s metabolic response to fat intake. We discuss a biophysical characterization of modulated synaptic communication in the slice following acute glucose and insulin stimulation, chronic elevation of insulin in mice that are in a conscious state, and induction of diet-induced obesity. We have discovered that Kv1.3 contributes an unusual nonconducting role – the detection of metabolic state.

## 1 Introduction

### 1.1 Kv1.3 Channel Distribution and Function

The voltage-dependent potassium channel, Kv1.3, is a mammalian homolog of the *Shaker* subfamily of potassium channels, which has a selective distribution within the nervous

system including high expression in the dentate gyrus, the olfactory bulb, and the olfactory cortex (Kues and Wunder 1992). The biophysical properties of the channel were first described as characterized in T lymphocytes (Cahalan et al. 1985), where today, active drug discovery efforts to find the most effective molecules to block the vestibule of the channel remain a focus of intensive research designed to dampen inflammatory responses associated with degenerative diseases, principally multiple sclerosis (Cahalan and Chandy 2009). Although, classically, one envisions potassium channels as dampeners of excitability through timing of the interspike interval (ISI) and shape of the action potential, as well as drivers for setting the resting membrane potential (Jan and Jan 1994; Yellen 2002), recent data have demonstrated that this particular potassium channel has a plethora of nonconductive functions that make it highly unusual, or at least untraditional (Kaczmarek 2006). One of the reasons that Kv1.3 may have multiple regulatory roles could be attributed to its structure and favorability as a central scaffold upon which signaling molecules build protein–protein interactions. Kv1.3 has 17 tyrosine residues, several of which lie within good recognition motifs for tyrosine phosphorylation (Pawson 1995; Haganir and Jahn 2000). Site-directed mutagenesis has been applied to both the channel and predicted regulatory kinases and adaptor proteins to map signaling cascades, associated with modulating channel function (Holmes et al. 1996a, b; Bowlby et al. 1997; Fadool et al. 1997; Fadool and Levitan 1998; Cook and Fadool 2002; Colley et al. 2004, 2007, 2009; Marks and Fadool 2007). For example, the cellular tyrosine kinase, src, phosphorylates residues Tyr<sup>137</sup> and Tyr<sup>449</sup> and has been found to substantially suppress Kv1.3 current, while slowing the kinetics of inactivation (Cook and Fadool 2002), while the receptor-linked epidermal growth factor receptor phosphorylates only Tyr<sup>479</sup> and predominantly acts to speed the kinetics of inactivation with only minor reduction in current amplitude (Bowlby et al. 1997). In the olfactory bulb, Kv1.3 is a substrate for phosphorylation by the insulin receptor kinase, whereby stimulation with the ligand insulin evokes no change in kinetic properties of the channel, but a reduction in current magnitude attributed to a reduction in mean open probability and not unitary conduction (Fadool and Levitan 1998; Fadool et al. 2000).

The discovery of the many nonconductive roles for Kv1.3 was made through loss of function studies using a whole-animal, targeted deletion of the Kv1.3 gene (Koni et al. 2003). Other laboratories including us noticed that the Kv1.3-null mice were thinner than their wild-type counterparts without caloric self-restriction (Fig. 1a and b) (Xu et al. 2003, 2004; Fadool et al. 2004). Using a custom designed metabolic chamber to quantify systems physiology parameters and ingestive behaviors (Fig. 3a–b) (Williams et al. 2003), we found that the Kv1.3-null animals, more frequently broke a photobeam that guarded access to their food receptacles (Fig. 1c), and oppositely, less frequently attended the water on a lick-o-meter (data not shown), while still maintaining identical total calorie and water intake as that of wild-type animals. The null animals had a slightly elevated metabolic activity and an increased locomotor activity particularly in the dark cycle (Fadool et al. 2004). Interestingly, Hennige et al. (2009) has demonstrated that the i.c.v. injection of the Kv1.3 pore blocker, margatoxin, similarly elevates locomotor activity and increases cortical action potential frequency.

Since Kv1.3 carries 60–80% of the outward current in the olfactory bulb primary output neurons (Fadool and Levitan 1998; Colley et al. 2004), the mitral cells, we were intrigued to explore olfactory-related phenotypes in the gene-targeted deleted models. By breeding the Kv1.3-null mice, onto a background of mice with a genetic marker for particular classes of odorant receptor-identified olfactory sensory neurons, we were able to discern that the projections of neurons into the olfactory bulb no longer converged to a single glomerular synaptic unit, but rather were supernumerary in target (Fig. 1d) (Biju et al. 2008). Within a given glomerulus, subsequent dual-color fluorescent confocal microscopy studies

demonstrated that glomeruli were no longer homogenous, but rather contained sensory projections from more than one class of olfactory sensory neurons (Biju et al. 2008). Behaviorally, the Kv1.3-null mice, had an increased olfactory ability in terms of both discrimination of molecular features of odorants, determined by odor-habituation trials (Fig. 1e) and in terms of odorant threshold, determined by the two-choice paradigm (Fadool et al. 2004).

## 2 Mechanistic Link Between Kv1.3 Ion Channel, Metabolism, and Olfaction

Given the world-wide health epidemic of the rise of the incidence of type II diabetes and unwanted weight gain (obesity), we immediately sought to determine the relationship between metabolic disorders, energy homeostasis, the modulation of this channel by insulin, and olfaction. We decided to challenge the Kv1.3-null animals, with a moderately high fat (MHF; 32% fat) diet for a period of 26 weeks and quantify body weight gain, serum chemistry, and metabolic profile as previously described by Tucker et al. (2008). Unlike wild-type counterparts, Kv1.3-null animals did not deposit significant quantities of fat in typical locations and were resistant to increases in body weight over the test interval (Fig. 2d). Wild-type animals demonstrated the induction of prediabetic blood chemistry (Fig. 2a), unlike that of Kv1.3-null animals, in which basal and fat challenged fasting glucose, serum insulin, and serum leptin levels were significantly reduced (data not shown). Using intranasal insulin delivery across the cribiform plate, into the olfactory bulb, we demonstrated that animals maintained on a MHF-diet now failed to exhibit an increase in insulin-induced Kv1.3 phosphorylation, developing a degree of insulin resistance at the level of the ion channel (Fig. 2b) (Marks et al. 2009). When genetically-identified odor receptor tagged mice were placed on a MHF-diet, and then a number of OR-specified olfactory sensory neurons were counted across the whole epithelia, we found that there was a loss of half of the neurons, or more directly, half the potential olfactory sensory information being received and relayed to the Kv1.3-containing postsynaptic targets, the mitral cell neurons (Fig. 2c).

To determine if the loss of Kv1.3, in the olfactory bulb and the resulting enhanced olfactory ability were responsible for the resistance to diet-induced obesity, we performed bilateral olfactory bulbectomy (OBX). Wild-type and Kv1.3-null animals underwent OBX (or sham) surgery by bilateral removal of the olfactory bulbs at 9 weeks of age as described by Getchell et al. (2005). Following a 2 week recovery from surgery, animals were placed on either control Purina diet or MHF regime for 5–6 weeks and then monitored for 8 days in the custom-housed metabolic chambers (Fig. 3a–b). At the end of the 16 week study, mice were behaviorally confirmed to be anosmic and then sacrificed to anatomically confirm complete bulb removal (Fig. 3c). If an OBX-treated animal was found to be able to detect a buried food item or more than 25% of the bulb remained (Fig. 3d), the data for that animal was excluded from the data set for analysis. Quite remarkably, OBX-treated, Kv1.3-null animals were no longer able to abrogate weight gain following maintenance on the MHF-diet (Fig. 3f). Figure 3e demonstrates weight gain in OBX-treated wild-type animals in comparison (Fig. 3e). Metabolic assessment determined that both control and MHF-diet fed Kv1.3-null treatment groups transiently increased caloric intake following bulbectomy, whereas wild-type animals, did not. In particular, MHF-diet challenged Kv1.3-null mice increased their basal metabolic rate. Combined removal of the olfactory bulb and maintenance on the MHF-diet, was found to decrease activity-dependent metabolic rate and thereby decrease total weight-dependent energy expenditure computed using the Weir equation (Weir 1949). These data directly demonstrate that the olfactory bulb contributes to the metabolic balance of energy usage; a brain region outside of the traditional hypothalamic pituitary, endocrine axis.

### 3 Modulation of Kv1.3 by Metabolically Important Molecules

If gene-targeted deletion of Kv1.3 channel evokes a thin, supersmeller phenotype that is resistant to diet- and genetically-induced obesity, and maintenance of wild-type mice on high fat diets with presumably elevated glucose and insulin levels decreases the number of olfactory sensory neurons, then, what is the functional ramification at the level of electrical excitability for the mitral cell; a major contributor of Kv1.3 conductance in the olfactory bulb? We had previously reported biochemical evidence that Kv1.3 was a substrate for phosphorylation by insulin using a heterologous expression system (Fadool and Levitan 1998), and thus used this same system to determine if glucose also could modulate Kv1.3 biophysics. In order to test whether two metabolically important molecules – insulin and glucose – modulated Kv1.3 in vivo, it was essential for us to additionally develop an adult olfactory bulb slice preparation so that we could explore modulation after chronic stimulation with these molecules (i.e., intranasal delivery approaches) or following induction of diet-induced obesity (i.e., maintenance on a MHF-diet since birth).

#### 3.1 Glucose

Acute glucose sensitivity of olfactory bulb mitral cells was evaluated by whole-cell current-clamp recordings from horizontal sections (325  $\mu\text{m}$ ) prepared from C57BL/6 mice (wildtype) or mice with a Kv1.3 gene-targeted deletion (Kv1.3-null). Mitral cell membrane potentials were held at  $-65$  mV to prevent spontaneous spiking followed by a 4 s, perithreshold (50–100 pA) current injection every 20 s during treatment with artificial cerebral spinal fluid (ACSF) containing 0 mM  $\text{D}$ -glucose with 22 mM  $\text{D}$ -mannitol osmotic balance for 10 min followed by 22 mM  $\text{D}$ -glucose and 0 mM  $\text{D}$ -mannitol for 10 min. During these experiments, we observed two populations of glucose sensitive mitral cells from wild-type animals based on changes in total spiking frequency. Forty-eight percent of mitral cells tested, exhibited an increased spiking frequency in response to changing the glucose concentration of the extracellular bath from 0 to 22 mM  $\text{D}$ -glucose and were therefore considered to be glucose excited. The other 52% exhibited a drop in spiking frequency, or were glucose inhibited, in the presence of 22 mM  $\text{D}$ -glucose. Mitral cells from Kv1.3-null mice, however, exhibited no change in spiking frequency due to change in glucose concentration. This suggests that Kv1.3 expression is important, at least in part, for glucose sensitivity of mitral cells.

#### 3.2 Insulin

Acute application of insulin to mitral cells shortens the ISI as determined through the Gaussian fitting of ISI histograms generated from action potentials evoked from current injections stepped from 25 to 500 pA in cells held near the resting membrane potential. Mitral cell firing frequency linearly increased from 10 to approximately 45 Hz over current steps ranging from 25 to 200 pA. Following acute insulin stimulation of the slice for 20 min, the firing frequency significantly increased from 25 to 60 Hz in response to the same current steps. Interestingly, at stronger current injections, ranging from 300 to 500 pA, firing frequency in untreated mitral cells progressively fell below 45 Hz due to spike adaptation, but following acute insulin stimulation, mitral cells could maintain firing rates up to 85 Hz without adaptation. Spike shape was significantly modified following acute insulin stimulation, whereby the action potential width was reduced, the action potential amplitude was increased, and the spike decay time ( $1/e$ ) was faster. At perithreshold current injections (5–30 pA) using long duration current steps (5,000 ms) we found that the characteristic spike clustering generated by mitral cells was modified following acute insulin stimulation. Spike clustering is due to intrinsic membrane properties, persists in the presence of NBQX and APV synaptic blockers, and is thought to provide frequency information for odorant discrimination (Balu and Strowbridge 2007). We found that the pause duration of the spike

clusters was significantly decreased following insulin stimulation. If insulin were delivered chronically as opposed to acutely, then a different pattern of spike clustering was observed. We intranasally delivered insulin, twice a day for 8 days, as per Marks et al. (2009), to P50 and older animals, and then measured generated action potentials evoked at perithreshold current injections. Following chronic insulin treatment, mitral cells exhibited two basal types of firing frequencies that were discreetly opposite in graphed activity patterns using raster plots. Basally, neurons either had extremely high levels of spike clusters with short pause durations, or neurons fired with short latency to first action potential spike and only a single spike cluster of short duration was observed. Following application of insulin to these slices, insulin now evoked a decrease in the action potential firing frequency, regardless of which initial pattern of activity was exemplified. Finally, mice that were placed on a MHF-diet via feeding the dam prior to pairing the parents, and then retaining weaned pups on the diet through adulthood (P35–P65), showed basal mitral cell properties that included modified timing of spike clusters, spike train adaption, and partial firing. Acute application of insulin to animals maintained on the MHF-diet, since birth was now ineffective in changing action potential firing frequencies.

## 4 Conclusion of Nonconductive Roles for Kv1.3 Governing Energy Homeostasis

We have demonstrated that disruption of the Kv1.3 gene, results in reduced body weight, abrogation of obesity, modified axonal targeting in the olfactory system, increased olfactory ability, and changes in serum blood chemistry. Maintenance on a moderately high-fat diet reduces the number of olfactory sensory neurons while elevating insulin and glucose that we have directly shown to alter mitral cell biophysical properties in a slice configuration of the olfactory bulb. A variant in the promoter of the Kv1.3 gene (i.e., gain in channel function), and referred to as the diabetes risk allele, has recently been associated with impaired glucose tolerance, lower insulin sensitivity, higher fasting plasma glucose, and impaired olfactory dysfunction in males (Tschritter et al. 2006; Guthoff et al. 2009). It appears that natural changes in the sensitivity of the OB driven by modulation of Kv1.3 (in rats and humans) may contribute to the body's metabolic response to fat intake or energy imbalance.

## Acknowledgments

We would like to thank Mr. Michael Henderson and Steven J. Godbey for routine technical assistance and mouse colony husbandry. We would like to thank Ms. Marita Madson for many insightful electrophysiological discussions. We would like to thank Mr. Charles Badland for artistic assistance in the visuals used in our oral presentation for this symposium. This work was supported by NIH grants R01 DC003387 & F31 DC010097 from the NIDCD, the Tallahassee Memorial Hospital/Robinson Foundation, and a Sabbatical Award from Florida State University.

## References

- Balu R, Strowbridge BW. Opposing inward and outward conductances regulate rebound discharges in olfactory mitral cells. *J Neurophysiol.* 2007; 97:1959–1968. [PubMed: 17151219]
- Biju KC, Marks DR, Mast TG, Fadool DA. Deletion of voltage-gated channel affects glomerular refinement and odorant receptor expression in the mouse olfactory system. *J Comp Neurol.* 2008; 506:161–179. [PubMed: 18022950]
- Bowlby MR, Fadool DA, Holmes TC, Levitan IB. Modulation of the Kv1.3 potassium channel by receptor tyrosine kinases. *J Gen Physiol.* 1997; 110:601–610. [PubMed: 9348331]
- Cahalan MD, Chandy KG. The functional network of ion channels in T lymphocytes. *Immunol Rev.* 2009; 231:59–87. [PubMed: 19754890]
- Cahalan MD, Chandy KG, DeCoursey TE, Gupta S. A voltage-gated potassium channel in human T lymphocytes. *J Physiol.* 1985; 358:197–237. [PubMed: 2580081]

- Colley B, Biju KC, Visegrady A, Campbell S, Fadool DA. TrkB increases Kv1.3 ion channel half-life and surface expression. *Neuroscience*. 2007; 144:531–546. [PubMed: 17101229]
- Colley B, Cavallin MA, Biju KC, Fadool DA. Brain-derived neurotrophic factor modulation of Kv1.3 channel is dysregulated by adaptor proteins Grb10 and nShc. *Neuroscience*. 2009; 144(2):531–546. [PubMed: 17101229]
- Colley B, Tucker K, Fadool DA. Comparison of modulation of Kv1.3 channel by two receptor tyrosine kinases in olfactory bulb neurons of rodents. *Receptors Channels*. 2004; 10:25–36. [PubMed: 14769549]
- Cook KK, Fadool DA. Two adaptor proteins differentially modulate the phosphorylation and biophysics of Kv1.3 ion channel by SRC kinase. *J Biol Chem*. 2002; 277:13268–13280. [PubMed: 11812778]
- Fadool DA, Holmes TC, Berman K, Dagan D, Levitan IB. Multiple effects of tyrosine phosphorylation on a voltage-dependent potassium channel. *J Neurophysiol*. 1997; 78:1563–1573. [PubMed: 9310443]
- Fadool DA, Levitan IB. Modulation of olfactory bulb neuron potassium current by tyrosine phosphorylation. *J Neurosci*. 1998; 18:6126–6137. [PubMed: 9698307]
- Fadool DA, Tucker K, Perkins R, Fasciani G, Thompson RN, Parsons AD, Overton JM, Koni PA, Flavell RA, Kaczmarek LK. Kv1.3 channel gene-targeted deletion produces “Super-Smeller Mice” with altered glomeruli, interacting scaffolding proteins, and biophysics. *Neuron*. 2004; 41:389–404. [PubMed: 14766178]
- Fadool DA, Tucker K, Phillips JJ, Simmen JA. Brain insulin receptor causes activity-dependent current suppression in the olfactory bulb through multiple phosphorylation of Kv1.3. *J Neurophysiol*. 2000; 83:2332–2348. [PubMed: 10758137]
- Getchell TV, Liu H, Vaishnav RA, Kwong K, Stromberg AJ, Getchell ML. Temporal profiling of gene expression during neurogenesis and remodeling in the olfactory epithelium at short intervals after target ablation. *J Neurosci Res*. 2005; 80(3):309–329. [PubMed: 15795924]
- Guthoff M, Tschritter O, Berg D, Liepelt I, Schulte C, Machicao F, Haering HU, Fritsche A. Effect of genetic variation in Kv1.3 on olfactory function. *Diabetes Metab Res Rev*. 2009; 25:523–527. [PubMed: 19489042]
- Hennige AM, Sartorius T, Lutz SZ, Tschritter O, Preissl H, Hopp S, Fritsche A, Rammensee HG, Ruth P, Häring H-U. Insulin-mediated cortical activity in the slow frequency range is diminished in obese mice and promotes physical inactivity. *Diabetologia*. 2009; 52:2416–2424. [PubMed: 19756482]
- Holmes TC, Fadool DA, Levitan IB. Tyrosine phosphorylation of the Kv1.3 potassium channel. *J Neurosci*. 1996a; 16:1581–1590. [PubMed: 8774427]
- Holmes TC, Fadool DA, Ren R, Levitan IB. Association of src tyrosine kinase with a human potassium channel mediated by SH3 domain. *Science*. 1996b; 274:2089–2091. [PubMed: 8953041]
- Huganir RL, Jahn R. Signalling mechanisms. *Curr Opin Neurobiol*. 2000; 10:289–292.
- Jan LY, Jan NJ. Potassium channels and their evolving gates. *Nature (London)*. 1994; 371:119–122. [PubMed: 8072541]
- Kaczmarek LK. Non-conducting functions of voltage-gated ion channels. *Nat Rev Neurosci*. 2006; 7:761–771. [PubMed: 16988652]
- Koni PA, Khanna R, Chang MC, Tang MD, Kaczmarek LK, Schlichter LC, Flavella RA. Compensatory anion currents in Kv1.3 channel-deficient thymocytes. *J Biol Chem*. 2003; 278:39443–39451. [PubMed: 12878608]
- Kues WA, Wunder F. Heterogeneous expression patterns of mammalian potassium channel genes in developing and adult rat brain. *Eur J Neurosci*. 1992; 4:1296–1308. [PubMed: 12106393]
- Marks DR, Fadool DA. Post-synaptic density 95 (PSD-95) affects insulin-induced Kv1.3 channel modulation of the olfactory bulb. *J Neurochem*. 2007; 103:1608–1627. [PubMed: 17854350]
- Marks DR, Tucker K, Cavallin MA, Mast TG, Fadool DA. Awake intranasal insulin delivery modifies protein complexes and alters memory, anxiety, and olfactory behaviors. *J Neurosci*. 2009; 29:6734–6751. [PubMed: 19458242]
- Pawson T. Protein modules and signalling networks. *Nature (London)*. 1995; 373(573–580):1995.

- Tucker K, Overton JM, Fadool DA. Kv1.3 gene-targeted deletion alters longevity and reduces adiposity by increasing locomotion and metabolism in melanocortin-4 receptor-null mice. *Int J Obes.* 2008; 32:1222–1232.
- Tschritter O, Machicao F, Stefan N, Schäfer S, Weigert C, Staiger H, Spieth C, Häring H-U, Fritsche A. A new variant in the human Kv1.3 gene is associated with low insulin sensitivity and impaired glucose tolerance. *J Clin Endocr Metab.* 2006; 91:654–658. [PubMed: 16317062]
- Weir JB. New methods for calculating metabolic rate with special reference to protein metabolism. *J Physiol.* 1949; 109:1–9. [PubMed: 15394301]
- Williams TD, Chambers JB, Gagnon SP, Roberts LM, Henderson RP, Overton JM. Cardiovascular and metabolic responses to fasting and thermoneutrality in Ay mice. *Physiol Behav.* 2003; 78:615–623. [PubMed: 12782216]
- Xu J, Koni PA, Wang P, Li G, Kaczmarek L, Wu Y, Li Y, Flavell RA, Desir GV. The voltage-gated potassium channel Kv1.3 regulates energy homeostasis and body weight. *Hum Mol Genet.* 2003; 12(5):551–559. [PubMed: 12588802]
- Xu J, Wang P, Li Y, Li G, Kaczmarek LK, Wu Y, Koni PA, Flavell RA, Desir GV. The voltage-gated potassium channel Kv1.3 regulates peripheral insulin sensitivity. *Proc Natl Acad Sci USA.* 2004; 101:3112–3117. [PubMed: 14981264]
- Yellen G. The voltage-gated potassium channels and their relatives. *Nature (London).* 2002; 419:35–42. [PubMed: 12214225]

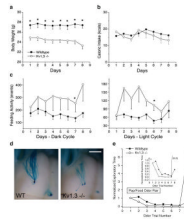


**Fig. 1.**

Loss of Kv1.3 gene causes a reduction in body weight, modified ingestive behaviors, disruption in axonal targeting in the olfactory bulb, and increased olfactory discrimination in mice. **(a)** Line graph of the mean  $\pm$  standard error of the mean (s.e.m.) bodyweight monitored for ten mice of each genotype. Wildtype = control C57B16 mice, Kv1.3<sup>-/-</sup> = mice with gene-targeted deletion of the Kv1.3 ion channel. **(b)** Line graph of the mean  $\pm$  s.e.m. caloric intake for ten mice of each genotype monitored for 8 days. **(c)** Line graph of the mean  $\pm$  s.e.m. feeding activity for ten mice of each genotype monitored for 8 days during the 12 h dark cycle (*left*) or 10 h of the light cycle (*right*). Computerized monitoring was disrupted for a 2 h interval/day for cage maintenance. *Asterisk* = significantly different by Student's *t*-test at the 95% confidence level. **(a–c)** Reproduced with permission from Fadool et al. (2004). **(d)** Axonal projections are visualized in a whole-mount of the olfactory bulb in M72*irestauLacZ* mice maintained on a wildtype (WT) or Kv1.3-null (Kv1.3<sup>-/-</sup>) background. Note the supernumerary glomerular projection in the Kv1.3-null animal at P20 that will remain unpruned through late adult (>2 years) (Biju et al. 2008). Scale bar = 1 mm. **(e)** Mice with a gene-targeted deletion (Kv1.3<sup>-/-</sup>) have an increased olfactory discrimination based upon enhanced performance in an odor-habituation paradigm. *Inset* = expanded Y axis to better visualize habituation phase **(a–c, e)**. Reproduced with permission from Fadool et al. (2004)

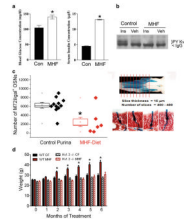


**Fig. 2.**

Mice maintained on a moderately high-fat (MHF) diet develop a prediabetic blood chemistry, resistance to Kv1.3 channel phosphorylation, and a loss of an OR-identified class of olfactory sensory neurons. Mice with a gene-targeted loss of Kv1.3 ion channel are resistant to obesity. **(a)** *Bar graph* of blood glucose and serum insulin concentrations for six wild-type mice maintained for 52 weeks on a control Purina chow (Con) or 32% fat diet (MHF). **(b)** Same cohort of mice in which mice were intranasally administered saline vehicle (Veh) or 0.1  $\mu$ g/ml insulin twice daily for 8 days. Proteins were immunoprecipitated with an antibody directed against Kv1.3 protein, separated by SDS-PAGE, and then probed with an antibody that recognizes tyrosine specific phosphorylation (PY Kv1.3). IgG = immunoglobulin band. **(c)** Combined scatter (each mouse) and box plot (population mean and s.e.m.) of the number of M72 B-galactosidase positive neurons in the epithelia of mice maintained on different dietary regimes. Same experimental diet paradigm was performed (as in **a** and **b**) on mice with a genetic marker for the M72 odorant receptor, *M72irestauLacZ*. Each whole epithelia were sectioned in entirety and then processed for  $\beta$ -galactosidase product to identify M72 expressing olfactory sensory neurons (OSNs). *Neutral red* was utilized as a counterstain (*right*) to better resolve OSNs in context. **(d)** *Bar graph* of the mean body weight  $\pm$  s.e.m. of wild-type (WT) or Kv1.3-null (Kv1.3<sup>-/-</sup>) mice maintained for 26 weeks on either the control Purina chow (CF) or 32% fat diet (MHF) (**a** and **b**). Reproduced with permission from Marks et al. (2009). **(c)** Whole-mount photograph modified with permission from Biju et al. (2008)

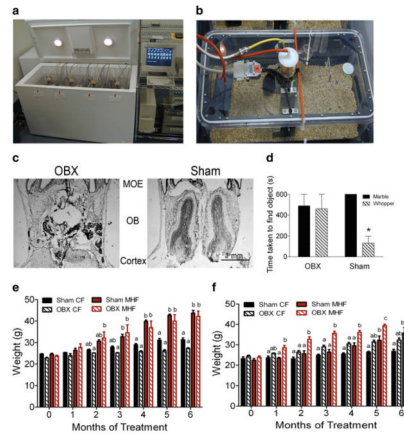


**Fig. 3.** Removal of the olfactory bulb in Kv1.3-null mice restores their sensitivity to diet-induced obesity via a reduction in energy expenditure. **(a)** Photograph showing the custom engineered metabolic chamber that is automated to collect respiratory quotient, locomotor activity, ingestive behavior every 30 s for 8 days while regulating circadian rhythms. **(b)** Close up photograph of the cage insert of the metabolic chamber that demonstrates how the cage is aerated, temperature regulated, and sealed to acquire indirect measures of calorimetry. **(c)** Photomicrograph of a 16  $\mu$ m thick coronal cyrosection through the olfactory bulb which was histologically stained to confirm complete surgical ablation of the olfactory bulb. **(d)** Bar graph of the mean  $\pm$  s.e.m. retrieval time for mice to uncover a scented object. OBX = mice with olfactory bulbectomy, SHAM = mice undergoing cranial surgery but bulb intact. **(e)** Bar graph of the mean  $\pm$  s.e.m. body weight for wild-type mice undergoing OBX or SHAM surgery and placed on a Purina control chow (CF) or 32% fat diet (MHF) for 14 weeks. **(f)** Same as panel e but for Kv1.3-null mice. Note: mice that were not visually confirmed as successfully ablated (panel c) or behaviorally anosmic (panel d), were not included in the weight study (panels e-f)